Stability condition of the steady oscillations in aggregation models with shattering process and self-fragmentation.

Jean-Yves Fortin, MooYoung Choi

Stability condition of the steady oscillations in aggregation models with shattering process and self-fragmentation

Jean-Yves Fortin[1] **and MooYoung Choi**[2]

[1] Laboratoire de Physique et Chimie Théoriques, CNRS UMR 7019,
Université de Lorraine, F-54000 Nancy, France
[2] Department of Physics and Astronomy and Center for Theoretical Physics
Seoul National University, Seoul 08826, Korea

E-mail: jean-yves.fortin@univ-lorraine.fr, mychoi@snu.ac.kr

Abstract. We consider a system of clusters of various sizes or masses, subject to aggregation and fragmentation by collision with monomers or by self-disintegration. The aggregation rate for the cluster of size (or mass) k is given by a kernel proportional to k^a with $a \geq 0$. The collision rate and the disintegration rate are given by λk^b and μk^b, respectively, with $0 \leq a, b \leq 1$ and positive factors λ and μ. We study the emergence of oscillations in the phase diagram (λ, μ) for two models: $(a, b) = (1, 0)$ and $(1, 1)$. It is shown that the monomer population satisfies a class of integral equations possessing oscillatory solutions in a finite domain in the plane (λ, μ). We evaluate analytically this domain in a precise way and give an estimate of the oscillation frequency. In particular, these oscillations are found to occur generally for small but nonzero values of the parameter μ, far smaller than λ.

PACS numbers: 05.20.Dd,05.45.-a,36.40.Qv,36.40.Sx

1. Introduction

The processes of aggregation and fragmentation between clusters of particles of various sizes or masses appear ubiquitous in a large variety of physical and chemical systems. Many examples found in the literature include the coalescence of soap bubbles, stability of atmospheric particles which aggregate due to the van der Waals forces, and large-scale internet networks where nodes acquire additional links according to their attachment preference weight [26, 1]. In astronomy, aggregation induced by gravitation plays an important role in forming planetary rings [2] and galactic clusters [3, 4]. Fragmentation by shattering, for example, tends to counterweight aggregation by preventing the masses of the clusters from becoming too large, and this often leads to an equilibrium state of the cluster size or mass distribution which displays a power law associated with an exponential decay [5, 6, 7, 8, 9, 10, 11]. Fragmentation can occur by a direct collision between large clusters, and the fragmentation rate depends on various parameters, such as the cross-section or masses of the objects. This also occurs indirectly by tidal forces between

large masses. Also, thermal fluctuations induce the disintegration of large polymers in solutions, which plays the role of self-fragmentation.

In the long-time limit, the steady state distribution of many models often exhibits, according to the type of kernel chosen for the aggregation or fragmentation processes, a power-law behavior associated with an exponential decay [5, 6, 12, 11, 13]. The exponent of the power-law decay is closely associated with the choice of the aggregation-fragmentation kernels, which depend on such parameters as the geometry of the clusters and their scattering cross-section.

Further, phase transitions can be observed while the kernel amplitudes vary. For example, in case only monomers or one-particle clusters interact with larger ones by aggregation and fragmentation, if the shattering rate is too small, the monomer population will vanish, and the dynamics will stop. The population of each cluster will therefore depend on the initial conditions. Otherwise, the distribution will reach a steady state [14]. In between, there is a critical regime depending on the amplitude and exponent values of the aggregation-fragmentation kernels where only giant clusters with large masses are created and where the population of other smaller ones tends to vanish asymptotically.

Besides time-independent equilibrium distributions of masses, one also observes collective and stable oscillations in a narrow window of parameter range [15, 16, 17, 18, 19, 20, 21, 22, 23]. This arises from non-equilibrium effects or imbalances between aggregation and fragmentation processes, with or without an external source of particles supplied to the system.

In a recent publication [20], oscillations were observed in a model where aggregation between monomers and clusters of size k occurs with rate $A_k = k$, as well as self-disintegration process with rate μk^b. They observed oscillations in a domain where μ is smaller than 10^{-6} and exponent

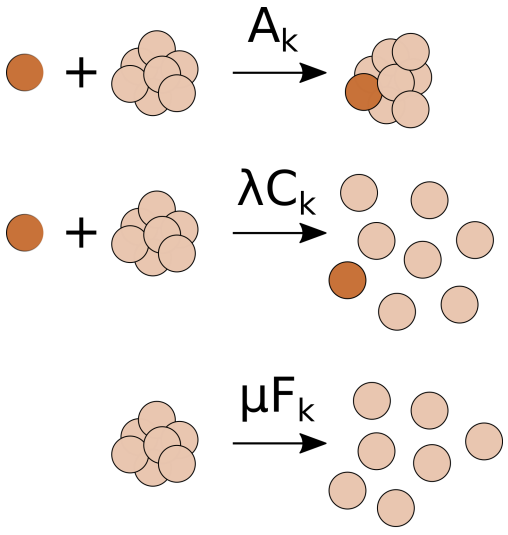

Figure 1: Aggregation, fragmentation, and disintegration processes in the model. A monomer collides and aggregates with a k-particle cluster with rate $A_k = k^a$, or fragments the cluster completely with rate $\lambda C_k = \lambda k^b$. Self-disintegration also occurs with rate $\mu F_k = \mu k^a$.

b smaller than 6 after linearizing the dynamical equations around the constant solution, reducing the problem to a linear algebra system. The stability of this infinite system is given by obtaining the set of complex eigenvalues after truncation, and the study of the sign of the real part of the eigenvalues close to the origin as well as the imaginary part characterizes the nature of the perturbation. The transition from stable to oscillatory solutions is often called Hopf bifurcation.

Usually, aggregation and fragmentation dynamics are described through Smoluchowski equations, which govern the fluctuations of the cluster masses. These Smoluchowski equations are quadratic in densities, and exact solutions may not be obtained in general, except for small sets of variables [24, 25] in the mathematical field of nonlinear systems of equations. In this case, it is difficult to characterize the presence of density oscillations. However, if clusters interact only with monomers, the dynamical equations can be simplified by rescaling all the densities and redefining time. All the properties of the dynamics can be deduced from an integral equation involving solely the distribution density of the monomers. This allows us to study analytically the oscillation behavior of the system in more detail. In case a source of the monomer is present, within some approximation, the monomer density satisfies a nonlinear ordinary differential equation (ODE) with a fluctuating damping term. This damping term is partially responsible for the Liénard oscillations that are observed: When the damping term is positive, the monomer density reduces toward zero. However, as the amplitude of the density gets very small, the damping term changes sign and encourages the density to grow again [23]. The presence of a source or even a self-fragmentation process constraints the monomer density to remain positive.

In this paper, we investigate a model restricted to dynamics driven by monomers, which is considered an extension of the Becker-Döring model [18, 22]. The dynamics include not only aggregation between monomers and larger clusters as well as fragmentation or shattering of clusters by collision with monomers but also self-fragmentation of clusters into monomers when they become too large. This is tantamount to total disintegration. The presence of self-fragmentation prevents the population of monomers from vanishing completely and the dynamics from stopping in a system where mass conservation holds. The three distinct processes, aggregation, fragmentation, and self-fragmentation, are included in this model, where the domain of stable oscillations is investigated. We would like particularly to develop a technical method applicable to the study of collective oscillations through differential equations satisfied by a class of generating functions. These generating functions contain all the moments of the densities, and in particular, we can extract precisely the monomer density, which determines all the other densities in a closed form. Computing eigenvalues in the analysis of the stability of the oscillations is replaced by finding zeroes of special functions in the complex plane.

The paper is organized as follows: Section 2 introduces the main model with general dynamics, from which two cases with different exponents are studied in detail. We present a method based on the differential equations satisfied by a generating function and display the phase diagram of the domain of oscillation stability as a function of the parameter amplitudes. In section 3, we discuss the general class of the obtained generating functions and integral equations for which

oscillating solutions exist. Finally, section 4 gives a brief conclusion of the present study.

2. Model

We consider a series of clusters made of k particles, each with a mass probability density n_k. Only one-particle clusters react with bigger clusters of size $k \geq 2$. A particle can aggregate with a cluster of size k to form a cluster of size $k+1$ with rate A_k. Or it can fragment the cluster completely to form k single particles with rate λC_k. The aggregation rate A_k grows with the cluster size k, according to a power law with exponent a, such that $A_k = k^a$. Similarly, the fragmentation rate is given by $\lambda C_k = \lambda k^b$ with $b \leq a$. Clusters of size k can spontaneously disintegrate into k monomers with rate $\mu F_k = \mu k^a$. All these processes are illustrated in figure 1. Normally the aggregation or self-fragmentation rates are proportional to the cluster size or surface, eventually fractal, and it is usual to take $0 \leq a \leq 1$, as observed for the problem of network growth [26]. Fragmentation exponent b will also be taken less than or equal to unity.

With N denoting the size of the largest cluster, we have the following master equations for the densities:

$$\begin{aligned}
\frac{\partial n_1}{\partial t} &= -2n_1^2 - \sum_{k=2}^{N-1}(A_k - \lambda k C_k)n_1 n_k + \lambda N C_N n_1 n_N + \sum_{k=2}^{N} \mu k F_k n_k, \\
\frac{\partial n_k}{\partial t} &= A_{k-1} n_1 n_{k-1} - (A_k + \lambda C_k) n_1 n_k - \mu F_k n_k \quad (2 \leq k \leq N-1), \\
\frac{\partial n_N}{\partial t} &= A_{N-1} n_1 n_{N-1} - \lambda C_N n_1 n_N - \mu F_N n_N.
\end{aligned} \tag{1}$$

These coupled equations satisfy the conservation of the total mass, set equal to unity: $\sum_{k=1}^{N} k n_k = 1$ or $\partial_t \sum_{k=1}^{N} k n_k = 0$. It is convenient to redefine the variables by introducing $v_k \equiv A_k n_k$ and effective time $\tau = \tau(t)$ such that $d\tau \equiv n_1(t)dt$. This leads to a set of quasi-linear ODEs:

$$\begin{aligned}
\frac{\partial v_1}{\partial \tau} &= -2v_1 - \sum_{k=2}^{N-1}(1 - \lambda k^{1+b-a})v_k + \lambda N^{1+b-a} v_N + \sum_{k=2}^{N} \mu k \frac{v_k}{v_1}, \\
\frac{\partial v_k}{\partial \tau} &= k^a v_{k-1} - (k^a + \lambda k^b) v_k - \mu k^a \frac{v_k}{v_1} \quad (2 \leq k \leq N-1), \\
\frac{\partial v_N}{\partial \tau} &= N^a v_{N-1} - \lambda N^b v_N - \mu N^a \frac{v_N}{v_1}.
\end{aligned} \tag{2}$$

2.1. Model with $(a, b) = (1, 0)$

In this section, we choose the parameters $(a, b) = (1, 0)$ and take the limit $N \to \infty$. Then the master equations read

$$\frac{\partial v_1}{\partial \tau} = -2v_1 - \sum_{k \geq 2}(1 - \lambda)v_k + \sum_{k \geq 2} \mu k \frac{v_k}{v_1},$$

$$\frac{\partial v_k}{\partial \tau} = k v_{k-1} - (k+\lambda) v_k - \mu k \frac{v_k}{v_1} \quad (k \geq 2). \tag{3}$$

It is useful to define the set of moments: $\varphi_l \equiv \sum_{k\geq 2} k^l v_k$. Since the total mass is given by $\sum_{k=1}^{N} k n_k = \sum_{k=1}^{N} v_k = 1$, we have $\varphi_0 = 1 - v_1$ and write the first equation of equation (3) in the form: $\partial v_1/\partial \tau = \lambda - 1 - (1+\lambda) v_1 + \mu \varphi_1 / v_1$. The general system of ODEs for φ_l is given by

$$\frac{\partial \varphi_l}{\partial \tau} = -\left(1 + \frac{\mu}{v_1}\right) \varphi_{l+1} - \lambda \varphi_l + 2^{l+1} v_1 + \sum_{j=0}^{l+1} \binom{l+1}{j} \varphi_j, \tag{4}$$

for $l \geq 0$. We then introduce a generating function $G(u,\tau) \equiv \sum_{l\geq 0} \varphi_l u^l / l!$, which satisfies the partial differential equation (PDE)

$$\frac{\partial G(u,\tau)}{\partial \tau} + \left(1 + \frac{\mu}{v_1} - e^u\right) \frac{\partial G(u,\tau)}{\partial u} = (e^u - \lambda) G(u,\tau) + 2 e^{2u} v_1, \tag{5}$$

with the initial condition $G(u,0)$ depending on the initial cluster densities. Note that in the derivation of equation (5), we have used the formula

$$\sum_{l \geq \max[0, j-1]} \binom{l+1}{j} \frac{u^l}{l!} = \frac{u^{j-1}(u+j)}{j!} e^u. \tag{6}$$

This can be demonstrated using the Egorychev method and the representation of the binomial coefficient in terms of a complex integral with a closed contour around the origin:

$$\binom{l+1}{j} = \oint \frac{dz}{2i\pi z} \frac{(1+z)^{l+1}}{z^j}, \tag{7}$$

which reduces the summation over l in equation (6) to a simple complex integral evaluated as follows:

$$\sum_{l\geq 0} \binom{l+1}{j} \frac{u^l}{l!} = \oint \frac{dz}{2i\pi z} \frac{(1+z)}{z^j} e^{u(1+z)} = \frac{u^{j-1}(u+j)}{j!} e^u. \tag{8}$$

Now, to solve equation (5), we apply the Lagrange-Charpit method based on the characteristic curves. We parametrize u and τ by an external variable s, such that $(u(s), \tau(s))$ defines a curve on the surface $(u, \tau, G(u,\tau))$. The generating function becomes a function of s, which we denote $G(u(s), \tau(s)) \equiv \tilde{G}(s)$. The derivative $\tilde{G}'(s)$ is then given, via the chain rule, by $\tilde{G}'(s) = u'(s) \partial_u G(u(s), \tau(s)) + \tau'(s) \partial_\tau G(u(s), \tau(s))$. For convenience, we choose the variable s such that

$$\tau'(s) = 1 \text{ and } u'(s) = 1 + \frac{\mu}{v_1(\tau(s))} - e^{u(s)}. \tag{9}$$

These can be integrated into

$$\begin{aligned} &\tau(s) = s, \\ &u(s) = \int_0^s ds' \left[1 + \frac{\mu}{v_1(s')}\right] - \log\left[C + \int_0^s ds' \exp\left\{\int_0^{s'} ds'' \left[1 + \frac{\mu}{v_1(s'')}\right]\right\}\right], \end{aligned} \tag{10}$$

where C is a constant determined by the boundary conditions on the curve. Imposing here that the point (u, τ) belongs to the curve, i.e., $s = \tau$ and $u(\tau) = u$, we obtain the constant value

$$C = e^{\gamma(\tau)-u} - \int_0^\tau ds e^{\gamma(s)}, \tag{11}$$

where $\gamma(s) = s + \int_0^s ds' \mu v_1^{-1}(s')$. With such parametrization, (equation (5)) becomes a first-order ODE

$$\tilde{G}'(s) = (e^{u(s)} - \lambda)\tilde{G}(s) + 2e^{2u(s)} v_1(s), \tag{12}$$

which can be integrated into

$$\begin{aligned} \tilde{G}(s) &= 2e^{W(s)} \int_0^s ds' v_1(s') e^{-W(s')+2u(s')}, \\ W(s) &= \int_0^s ds' e^{u(s')} - \lambda s = \log\left[C + \int_0^s ds' e^{\gamma(s')}\right] - \log C - \lambda s. \end{aligned} \tag{13}$$

After simplifying the previous expressions, we obtain $\tilde{G}(s)$ in the form

$$\begin{aligned} \tilde{G}(s) = 2 &\left\{ e^{-u} - \int_s^\tau ds'' \exp\left[s'' - \tau - \mu \int_{s''}^\tau ds''' v_1^{-1}(s''') \right] \right\} \\ &\times \int_0^s ds' v_1(s') \frac{\exp\left[\lambda(s'-s) + 2(s'-\tau) - 2\mu \int_{s'}^\tau ds'' v_1^{-1}(s'')\right]}{\left[e^{-u} - \int_{s'}^\tau d\tau'' \exp\left[s'' - \tau - \mu \int_{s''}^\tau ds''' v_1^{-1}(s''')\right]\right]^3}. \end{aligned} \tag{14}$$

The initial conditions are chosen such that only monomers are present at $s = \tau = 0$ with the total mass unity, namely, $v_k(0) = \delta_{k1}$. This implies that $\tilde{G}(0) = G(u(0), 0) = 0$ since φ_l is initially zero for all l. Substituting $s = \tau$ and $u = 0$, we obtain an integral equation for $v_1(\tau)$. Indeed, we have $G(0, \tau) = \varphi_0 = \sum_{k\geq 2} v_k = 1 - v_1$ and therefore

$$v_1(\tau) = 1 - 2\int_0^\tau d\tau' v_1(\tau') \frac{\exp\left[-(2+\lambda)(\tau-\tau') - 2\mu \int_{\tau'}^\tau d\tau'' v_1^{-1}(\tau'')\right]}{\left[1 - \int_{\tau'}^\tau d\tau'' \exp\left\{\tau'' - \tau - \mu \int_{\tau''}^\tau d\tau''' v_1^{-1}(\tau''')\right\}\right]^3}. \tag{15}$$

2.1.1. Case $\mu = 0$. When $\mu = 0$, equation (15) can be simplified and reduces to

$$v_1(\tau) = 1 - 2\int_0^\tau d\tau' v_1(\tau') e^{-(\lambda-1)(\tau-\tau')}. \tag{16}$$

Taking the Laplace transform, we obtain, for $\lambda > 1$,

$$\hat{v}_1(p) = \frac{1}{p} \frac{\lambda - 1 + p}{\lambda + 1 + p}, \tag{17}$$

which gives a long-time constant $v_1(\tau) \simeq (\lambda - 1)/(\lambda + 1)$ as $p \to 0$. We can also differentiate equation (16) and eliminate the integral to obtain the ODE

$$v_1'(\tau) = -(1 + \lambda) v_1(\tau) + \lambda - 1, \tag{18}$$

which yields the time-dependent solution $v_1(\tau) = (\lambda - 1 + 2e^{-(\lambda+1)\tau})/(\lambda + 1)$. For $\lambda < 1$, v_1 decreases and vanishes at a finite time $\tau = (1 + \lambda)^{-1} \log[2/(1 - \lambda)]$.

2.1.2. Constant solution. Here we discuss the long-time constant solution of equation (15). Supposing that $v_1(\tau)$ reaches a limit v_1^* (> 0), we obtain the equation describing this solution for $\tau \gg 1$:

$$\begin{aligned} v_1^* &\simeq 1 - 2v_1^* \int_0^\tau d\tau' \frac{e^{-(2+\lambda+2\mu/v_1^*)(\tau-\tau')}}{\left[1 - \int_{\tau'}^\tau e^{-(1+\mu/v_1^*)(\tau-\tau'')} d\tau''\right]^3} \\ &\simeq 1 - 2v_1^*(1+\epsilon)^3 \int_0^\tau d\tau' \frac{e^{-(2+\lambda+2\epsilon)\tau'}}{\left[\epsilon + e^{-(1+\epsilon)\tau'}\right]^3}, \end{aligned} \tag{19}$$

where $\epsilon \equiv \mu/v_1^*$ is assumed small ($\epsilon \ll 1$) for small μ. When $\mu = 0$ or $\epsilon = 0$ and $\lambda > 1$, the integral in equation (19) is finite, and v_1 approaches exponentially to the constant solution $v_1^* = (\lambda - 1)/(\lambda + 1)$ as $\tau \to \infty$. Otherwise, for $\lambda < 1$, v_1 reaches zero at some finite time τ. For $\lambda = 1$, v_1 decays to zero with a power law. When $\mu \neq 0$, there is a finite nonzero solution to the integral equation (19) for any value of λ. Changing the variable $x = \epsilon^{-1} e^{-(1+\epsilon)\tau'}$ and taking the limit $\tau \to \infty$, we rewrite equation (19) as

$$v_1^* = \left[1 + 2(1+\epsilon)^2 \epsilon^{\frac{\lambda-1-\epsilon}{1+\epsilon}} \int_0^{1/\epsilon} dx \frac{x^{\frac{1+\lambda+\epsilon}{1+\epsilon}}}{(1+x)^3}\right]^{-1}. \tag{20}$$

The behaviour of the integral depends on λ when ϵ is small. If $\lambda > 1 + \epsilon$, the integral diverges for large x, and the dominant contribution comes from $x \simeq 1/\epsilon$ ($\gg 1$):

$$\int_0^{1/\epsilon} dx \frac{x^{\frac{1+\lambda+\epsilon}{1+\epsilon}}}{(1+x)^3} \simeq \frac{1+\epsilon}{\lambda - 1 - \epsilon} \epsilon^{\frac{1+\epsilon-\lambda}{1+\epsilon}}. \tag{21}$$

Combining this asymptotic result with equation (20), we obtain, for $\epsilon \ll 1$:

$$v_1^* = \left[1 + 2\frac{(1+\epsilon)^3}{\lambda - 1 - \epsilon}\right]^{-1} \simeq \frac{\lambda - 1}{\lambda + 1}, \tag{22}$$

which is the expected result for λ large compared with μ. If $\lambda < 1 + \epsilon$, then the integral converges in the limit $x \to \infty$:

$$\int_0^\infty dx \frac{x^{\frac{1+\lambda+\epsilon}{1+\epsilon}}}{(1+x)^3} = \frac{\pi\lambda(\lambda + 1 + \epsilon)}{2(1+\epsilon)^2 \sin[\pi\lambda/(1+\epsilon)]}, \tag{23}$$

which is a finite quantity. Therefore the dominant term in equation (20) is $\epsilon^{\frac{\lambda-1-\epsilon}{1+\epsilon}}$ ($\gg 1$), and some algebra leads to the approximate expression:

$$v_1^* \simeq \mu^{(1-\lambda)/(2-\lambda)} \left[\frac{\sin(\pi\lambda)}{\pi\lambda(\lambda+1)}\right]^{1/(2-\lambda)}, \tag{24}$$

for $\lambda < 1$ and $\mu \ll 1$. It is then straightforward to confirm that $\epsilon = \mu/v_1^* \propto \mu^{1/(2-\lambda)} \ll 1$.

2.1.3. Stability around the constant solution. Plotted in figures 2 and 3 are the time-dependent solutions of equation (2), obtained via the Runge-Kutta-Fehlberg (RKF45) algorithm, for $\mu = 10^{-5}$ and two different values of N. For small N ($= 1000$) steady oscillations are observed in a window

around $\lambda \simeq 0.6$ whereas for larger $N\,(= 10000)$ these oscillations are transient and tend to disappear, and $v_1(\tau)$ approaches its limiting value given by equation (20). This means that for finite N the system governed by equation (2), which conserves the total mass, displays steady oscillations depending on N. In the limit $N \to \infty$, however, these oscillations are not stable.

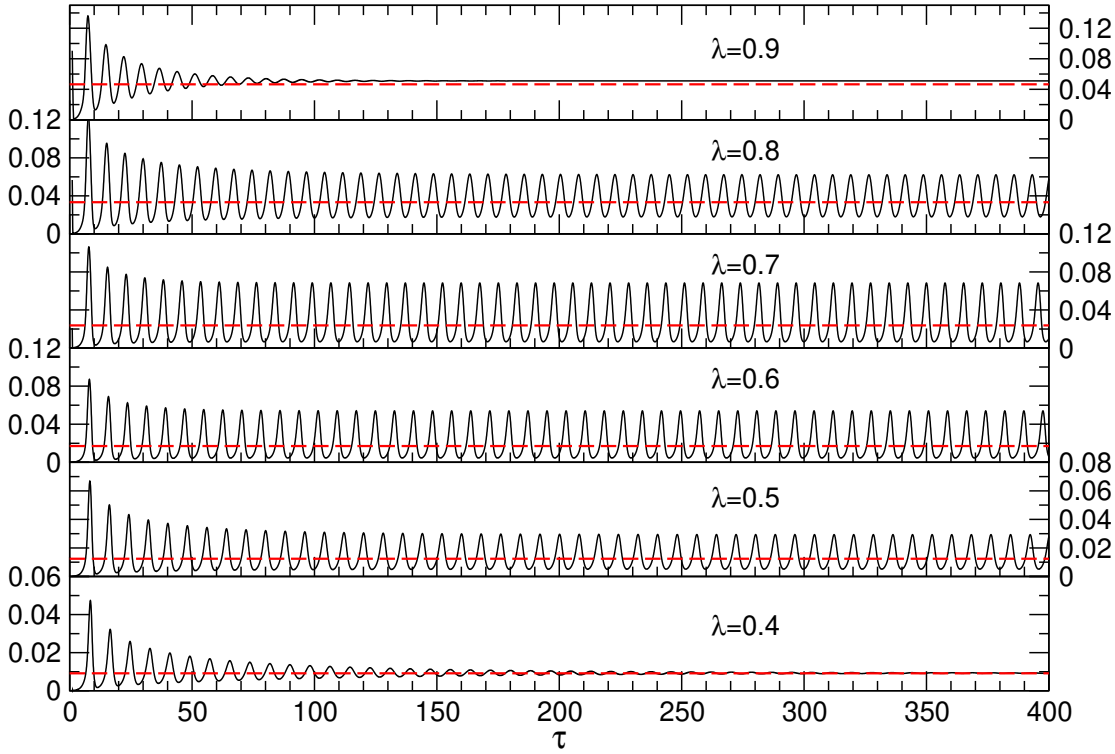

Figure 2: Time evolution of $v_1(\tau)$ for $\mu = 10^{-5}$, $N = 1000$, and several values of λ. For $\lambda \approx 0.6$, one observes steady oscillations around a mean value close to the constant solution v_1^* (dashed lines) given by equation (20).

In order to examine the stability, we consider a perturbation $\epsilon(\tau)$ and write $v_1(\tau) = v_1^* + \epsilon(\tau)$. Then linearization of equation (15) yields the integral equation for $\epsilon(\tau)$:

$$\epsilon(\tau) = -2\int_0^\tau d\tau' \frac{\epsilon(\tau')e^{-(2+\lambda+\mu/v_1^*)(\tau-\tau')}}{\left[1-\int_0^{\tau-\tau'} d\tau'' e^{-(1+\mu/v_1^*)\tau''}\right]^3} - \frac{2\mu}{v_1^*}\int_0^\tau d\tau' \frac{e^{-(2+\lambda+\mu/v_1^*)(\tau-\tau')}}{\left[1-\int_0^{\tau-\tau'} e^{-(1+\mu/v_1^*)\tau''} d\tau''\right]^3}$$
$$\times \left[2\int_{\tau'}^\tau d\tau''\epsilon(\tau'') + \frac{3\int_{\tau'}^\tau d\tau'' e^{-(1+\mu/v_1^*)(\tau-\tau'')}\int_{\tau''}^\tau d\tau'''\epsilon(\tau''')}{1-\int_0^{\tau-\tau'} d\tau'' e^{-(1+\mu/v_1^*)\tau''}}\right]. \quad (25)$$

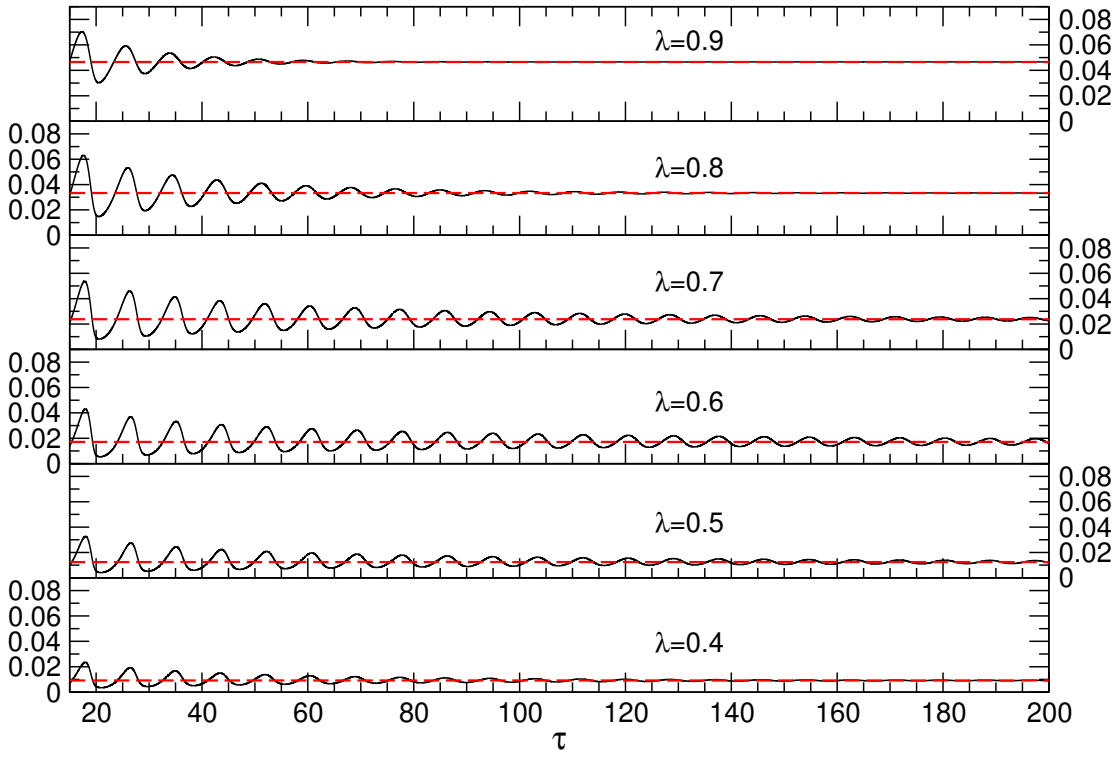

Figure 3: Time evolution of $v_1(\tau)$ for $\mu = 10^{-5}$, $N = 10000$, and several values of λ. The oscillations observed in figure 2 disappear, and the limiting value v_1^* (dashed lines) is reached asymptotically.

Note that the above does not take the form of an expansion in μ. Since there is no obvious convolution integral, we do not take a Laplace transform but consider a perturbation in the exponential form: $\epsilon(\tau) = \epsilon_0 e^{\Omega\tau}$ with ϵ_0 being a small amplitude. After some algebra, we obtain the equation for the complex frequency Ω:

$$1 + 2J_3(\beta{+}\Omega, \alpha) + \frac{2\mu}{\Omega v_1^*}\Big\{2\left[J_3(\beta, \alpha) - J_3(\beta{+}\Omega, \alpha)\right] + \frac{3}{\alpha}\left[J_4(\beta, \alpha) - J_4(\beta{+}\alpha, \alpha)\right] - \frac{3}{\alpha + \Omega}\left[J_4(\beta, \alpha) - J_4(\beta{+}\alpha{+}\Omega, \alpha)\right]\Big\} = 0, \tag{26}$$

where $\alpha \equiv 1 + \mu/v_1^*$, $\beta \equiv 2\alpha + \lambda$, and

$$J_k(\beta, \alpha) \equiv \alpha^k \int_0^\tau d\tau' \frac{e^{-\beta\tau'}}{(\alpha - 1 + e^{-\alpha\tau'})^k} \simeq \frac{\alpha^{k-1}}{(\alpha - 1)^{k-\beta/\alpha}} \int_0^{(\alpha-1)^{-1}} dx \frac{x^{\beta/\alpha - 1}}{(1 + x)^k}$$

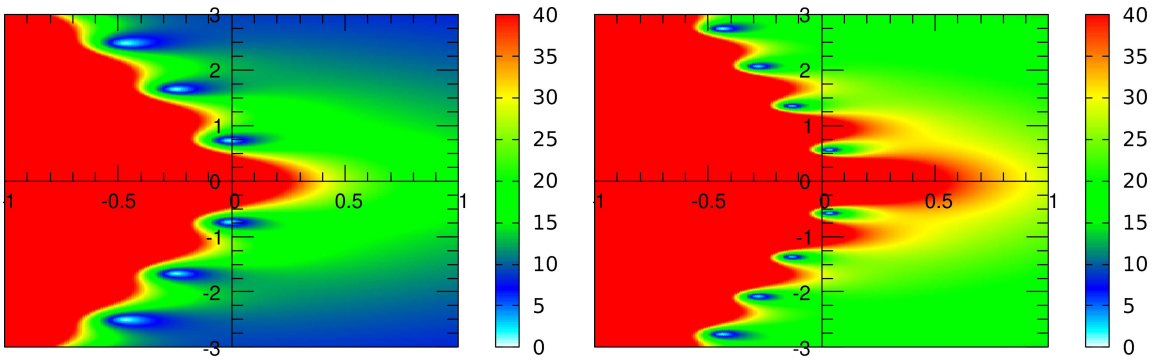

(a) (b)

Figure 4: Surface plots of the modulus of equation (26) in the complex Ω-plane $(\mathrm{Re}\,\Omega, \mathrm{Im}\,\Omega)$, for $\lambda = 0.6$ and $\mu =$ (a) 10^{-5} and (b) 10^{-6}. In (a), all the zeros located on the left part of the plane have negative real parts and therefore no oscillatory solution can occur except for transient oscillations in the case of the zeros close to the vertical axis. In (b), one conjugate pair of zeros has a small positive real part, giving rise to oscillations.

$$= \left(\frac{\alpha}{\alpha-1}\right)^{k-1}\left[(-1)^{k+1}\frac{\pi\Gamma(\beta/\alpha)(\alpha-1)^{\beta/\alpha-1}}{\Gamma(k)\Gamma(1+\beta/\alpha-k)\sin(\pi\beta/\alpha)} - \frac{\alpha(\alpha-1)^{k-1}{}_2F_1(k,k-\beta/\alpha;1-\beta/\alpha+k;1-\alpha)}{k\alpha-\beta}\right]. \tag{27}$$

Here the second integral has been obtained in the limit $\tau \to \infty$. Accordingly, this approximation should be valid for $|\Omega|\tau \gg 1$. The function J_k satisfies the following recursion relation

$$J_{k+1}(\beta,\alpha) = -\frac{1}{k} + \frac{\beta-\alpha}{k}J_k(\beta-\alpha,\alpha) \quad (\beta > \alpha > 1),$$
$$J_k(\alpha,\alpha) = \frac{1}{k-1}\left[\left(\frac{\alpha}{\alpha-1}\right)^{k-1} - 1\right] \quad (k > 1,\ \alpha > 1). \tag{28}$$

Figure 4 presents the modulus of equation (26) for $\lambda = 0.6$ and $\mu =$ (a) 10^{-5} and (b) $= 10^6$. The zeros are distributed on the left part of the complex plane, with negative real parts, except for the case (b), where one pair of complex conjugate has a slightly positive real part. Plotted in figure 5 is the solution that has the largest real part for various values of μ, as a function of λ. For μ smaller than 8×10^{-6}, the real part becomes positive around $\lambda \simeq 0.6$, and oscillations occur with the frequency given by the imaginary part of the solution, see figure 5(b).

The oscillations can be seen for $\lambda = 0.6$ in figure 6, where they are stable below $\mu < 8 \times 10^{-6}$. For $\mu = 8\times10^{-6}$, they are damped slowly as τ grows large, since the real part of the corresponding Ω is negative but close to zero. Figure 7 exhibits the phase diagram in the plane (λ, μ) corresponding to stable oscillations. The domain is bounded by $0 < \lambda < 1$ and $0 < \mu < 8 \times 10^{-6}$, with the case $\mu = 0$ excluded since it has $v_1(\tau)$ vanish at a finite time before any oscillation occurs. Carrying

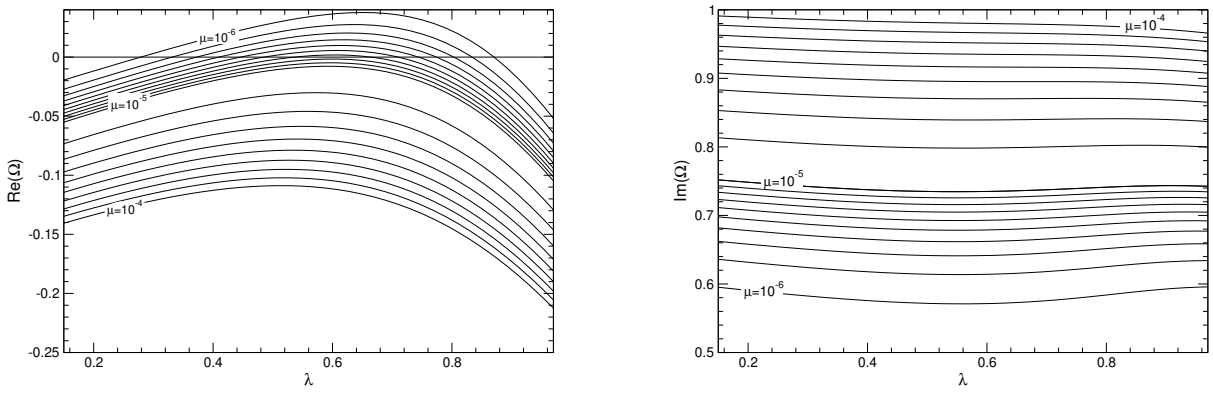

(a) (b)

Figure 5: (a) Plots of (a) the real part and (b) the imaginary part of the solution of equation (26) having the largest real part versus λ, for various values of μ.

out the Fourier transform of the signals in figure 6 for μ corresponding to the oscillatory solutions, we extract the frequency $\Omega_{\rm num}$ and present the obtained values in Table 1. These values are compared with the imaginary parts of the solutions of equation (26). It is observed that the differences are small when μ is close to the oscillation threshold. They tend to increase as μ is decreased or as the oscillation amplitude is increased. This presumably reflects the fact that the exponential growth of the signal is compensated by a fluctuating damping factor, as in the Liénard oscillations [23], which modifies the frequency slightly.

Table 1: Frequency $\Omega_{\rm num}$ for $\lambda = 0.6$ and several values of μ, extracted from the Fourier transform of the time oscillations in figure 6. For comparison, the imaginary part ImΩ of the solution of equation (26) is also given.

μ	$\Omega_{\rm num}$	$\mathrm{Im}\,\Omega$
1×10^{-6}	0.571	0.601
2×10^{-6}	0.614	0.620
4×10^{-6}	0.662	0.658
6×10^{-6}	0.692	0.690

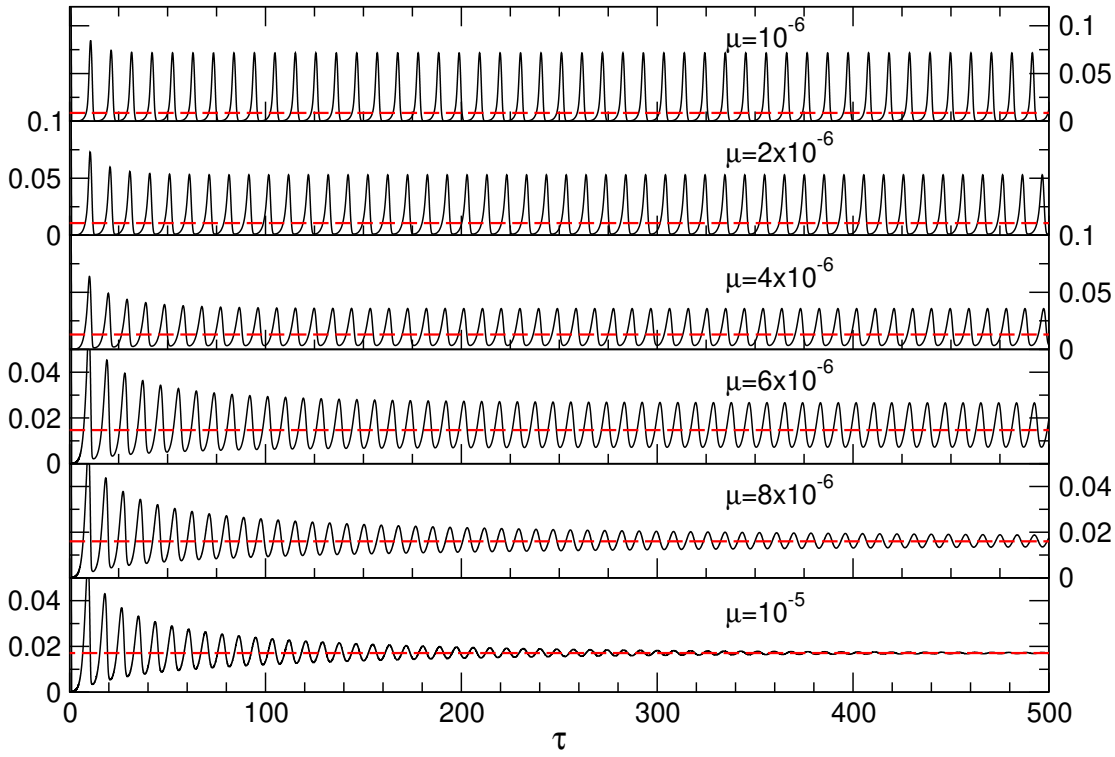

Figure 6: Oscillations for $\lambda = 0.6$ and several values of μ.1 For $\mu = 10^{-5}$ and 8×10^{-6}, oscillations are damped while v_1 approaches the limit given by equation (20) (red dashed lines).

2.2. Model with $(a, b) = (1, 1)$

In this section, we consider the case $(a, b) = (1, 1)$. As before, equation (2) leads to a linear PDE for the generating function $G(u, \tau)$, similar to equation (5):

$$\frac{\partial G(u,\tau)}{\partial \tau} + (1 + \lambda + \mu v_1^{-1} - e^u)\frac{\partial G(u,\tau)}{\partial u} = e^u G(u,\tau) + 2e^{2u} v_1. \tag{29}$$

The solution can be obtained via parametrizing u and τ such that $\tilde{G}(s) = G(u(s), \tau(s))$ with

$$\tau'(s) = 1 \quad \text{and} \quad u'(s) = 1 + \lambda + \frac{\mu}{v_1(\tau(s))} - e^{u(s)}, \tag{30}$$

which is integrated into

$$\tau(s) = s, \tag{31}$$

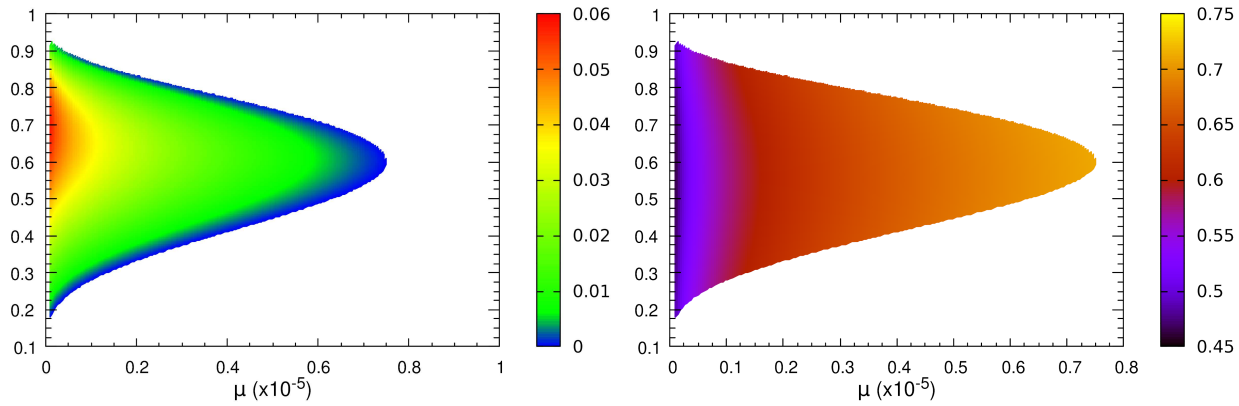

(a) (b)

Figure 7: (a) Plots of the (a) real and (b) imaginary parts of the solution of equation (26) with the largest real part, providing the phase diagram in the plane (λ, μ).

$$u(s) = \int_0^s ds' \left[1 + \lambda + \frac{\mu}{v_1(s')}\right] - \log\left[C + \int_0^s ds' \exp\left\{\int_0^{s'} ds''[1 + \lambda + \mu v_1^{-1}(s'')]\right\}\right].$$

Here C is a constant determined by the condition that the point (u, τ) belongs to the curve, namely, $s = \tau$ and $u(\tau) = u$, which gives

$$C = \exp\left[\gamma(\tau) - u\right] - \int_0^\tau ds \exp\left[\gamma(s)\right], \tag{32}$$

with $\gamma(s) \equiv (1 + \lambda)s + \int_0^s ds' \mu v_1^{-1}(s')$. The PDE (5) therefore reduces to

$$\tilde{G}'(s) = e^{u(s)}\tilde{G}(s) + 2e^{2u(s)}v_1(s), \tag{33}$$

which can be integrated into

$$\tilde{G}(s) = 2e^{W(s)} \int_0^s ds' v_1(s') e^{-W(s') + 2u(s')},$$
$$W(s) = \int_0^s ds' e^{u(s')} = \log\left[C + \int_0^s ds' e^{\gamma(s')}\right] - \log C. \tag{34}$$

Simplifying and using $G(0, \tau) = 1 - v_1(\tau)$, we obtain an implicit integral equation for $v_1(\tau)$:

$$v_1(\tau) = 1 - 2\int_0^\tau d\tau' \frac{v_1(\tau') \exp\left[-2(1 + \lambda)(\tau - \tau') - 2\mu \int_{\tau'}^\tau d\tau'' v_1^{-1}(\tau'')\right]}{\left\{1 - \int_{\tau'}^\tau d\tau'' \exp\left[(-(1 + \lambda)(\tau - \tau'') - \mu \int_{\tau''}^\tau d\tau''' v_1^{-1}(\tau''')\right]\right\}^3}, \tag{35}$$

which is similar to equation (15) except for the extra λ term in the exponential rates.

2.2.1. Case $\mu = 0$. In the case $\mu = 0$, equation (35) obtains the simple form

$$v_1(\tau) = 1 - 2\int_0^\tau d\tau' \frac{v_1(\tau') e^{-2(1+\lambda)(\tau - \tau')}}{\left[1 - \int_0^{\tau - \tau'} e^{-(1+\lambda)\tau''} d\tau''\right]^3}, \tag{36}$$

which can be solved by means of the Laplace transform:

$$\hat{v}_1(p) = \frac{1}{p}\frac{1}{1+2\hat{F}(p)}, \tag{37}$$

with $\hat{F}(p) = (1+\lambda)^2\lambda^{p/(1+\lambda)-1}\int_0^{1/\lambda} dx x^{1+p/(1+\lambda)}(1+x)^{-3}$. This results in

$$\hat{v}_1(p) = \frac{\sin\left(\pi\frac{p}{\lambda+1}\right)}{p(p+\lambda+1)\left\{\pi p\lambda^{\frac{p}{\lambda+1}-1} - \sin\left(\pi\frac{p}{\lambda+1}\right)\left[p\Phi\left(-\lambda,1,1-\frac{p}{\lambda+1}\right)+1\right]\right\}}, \tag{38}$$

where the Lerch transcendent function is defined by the formal series $\Phi(z,s,a) = \sum_{k\geq 0} z^k(k+a)^{-s}$. This solution possesses a long-time limit $\hat{v}_1(p) \simeq p^{-1}\lambda(1+\lambda)^{-1}$ as $p \to 0$, and therefore $v_1(\tau)$ approaches the constant value $v_1(\tau) \to v_1^* = \lambda(1+\lambda)^{-1}$. However, for λ small enough, $v_1(\tau)$ becomes negative before reaching the asymptotic value. By solving equation (2) numerically for, e.g., $N = 10000$, we find that for $\lambda < \lambda_c \simeq 0.16775$, the dynamics stops at a finite time τ when v_1 becomes negative. On the other hand, for $\lambda > \lambda_c$, the densities reach the equilibrium state where $v_1(\tau) = v_1^*$, and the other values ($k \geq 2$) decrease exponentially as

$$v_k = \frac{\lambda}{(\lambda+1)^k}, \tag{39}$$

see equation (40) below. Another method is to solve equation (2) for $(a,b) = (1,1)$ and $\mu = 0$. This yields the following system of equations:

$$\frac{\partial v_1}{\partial \tau} = -2v_1 - \sum_{k=2}^{\infty}(1-\lambda k)v_k,$$
$$\frac{\partial v_k}{\partial \tau} = kv_{k-1} - k(1+\lambda)v_k \quad (k \geq 2).$$

Taking the Laplace transform, we obtain recursively

$$\left[\lambda\sum_{k=2}^{\infty}\frac{k!k}{\prod_{j=2}^{k}[p+j(1+\lambda)]} - 1 - p\right]\hat{v}_1(p) = \frac{1}{p} - 1,$$
$$\hat{v}_k(p) = \prod_{j=2}^{k}\left[\frac{j}{p+j(1+\lambda)}\right]\hat{v}_1(p) \quad (k \geq 2). \tag{40}$$

The summation in the first expression can be reduced to a hypergeometric function as

$$\sum_{k=2}^{\infty}\frac{k!k}{\prod_{j=2}^{k}[p+j(1+\lambda)]} = \sum_{k=1}^{\infty}\frac{\Gamma(k+2)\Gamma(k+2)}{\Gamma(k+2+p/(\lambda+1))\Gamma(k+1)}(\lambda+1)^{-k}$$
$$= {}_2F_1\left(2,2;2+\frac{p}{\lambda+1};\frac{1}{\lambda+1}\right) - 1, \tag{41}$$

which in turn leads to

$$\left[\lambda\,{}_2F_1\left(2,2;2+\frac{p}{\lambda+1};\frac{1}{\lambda+1}\right) - \lambda - 1 - p\right]\hat{v}_1(p) = \frac{1}{p} - 1. \tag{42}$$

This is formally equivalent to the expression in equation (38) and gives an identity between the hypergeometric function ${}_2F_1$ and the Lerch function Φ by eliminating $\hat{v}_1$.

2.2.2. Stability around the constant solution. We consider a perturbation ϵ around the constant solution v_1^* of equation (38) and set $\alpha = 1 + \lambda > 1$. We thus write $v_1(\tau) = v_1^* + \epsilon(\tau)$, where ϵ satisfies the following integral equation

$$\begin{aligned}\epsilon(\tau) = & -2\int_0^\tau d\tau' \frac{\epsilon(\tau')e^{-2\alpha(\tau-\tau')}}{\left(1-\int_0^{\tau-\tau'} e^{-\alpha\tau''}d\tau''\right)^3} = -2\alpha^3\int_0^\tau d\tau' \frac{\epsilon(\tau')e^{-2\alpha(\tau-\tau')}}{\left[\alpha-1-e^{-\alpha(\tau-\tau')}\right]^3} \\ = & -2\int_0^\tau d\tau'\epsilon(\tau')F(\tau-\tau'). \end{aligned} \tag{43}$$

The Laplace transform of this expression gives $\hat{\epsilon}(p)[1+2\hat{F}(p)] = 0$, which indicates that a non-zero solution for the perturbation is possible if there exists p satisfying

$$1 + 2\hat{F}(p) = \left[\frac{\pi p\lambda^{p/(1+\lambda)-1}}{\sin[\pi p/(1+\lambda)]} - 1 - p\Phi(-\lambda, 1, 1-p/(1+\lambda))\right](1+p+\lambda) = 0. \tag{44}$$

The zeros of the function $1 + 2\hat{F}(p)$ can be located by plotting the modulus $|1 + 2\hat{F}(p)|$ in the complex plane as in figure 8(a). The zeros and their conjugates are aligned in the negative real part of the plane, except for a few zeros whose real parts are strictly positive. Plotted in figure 8(b) are the real part and the positive imaginary part of the zero which has the largest real part. The real part is positive for all λ less than $\lambda^* \simeq 0.068538$. In this case the perturbation grows exponentially and oscillates with a frequency equal to the imaginary part $\mathrm{Im}\, p$. However, since $\lambda^* < \lambda_c$, the solution v_1 becomes negative, and the dynamics should stop before oscillations occur. As we will see below, the presence of any small value of μ will lead to oscillations with a positive value of v_1.

2.2.3. Constant solution for $\mu \neq 0$. Here we consider the long-time constant solution of equation (35) by assuming that $v_1(\tau)$ approaches the constant solution $v_1^* > 0$ in the limit $\tau \to \infty$. This solution should satisfy

$$v_1^* = 1 - 2v_1^*\int_0^\infty d\tau' \frac{e^{-2(1+\lambda+\mu/v_1^*)\tau'}}{\left[1-\int_0^{\tau'} e^{-(1+\lambda+\mu/v_1^*)\tau''}d\tau''\right]^3}, \tag{45}$$

which, upon integration, yields the quadratic equation for v_1^*:

$$(1+\lambda){v_1^*}^2 + (\mu-\lambda)v_1^* - \mu = 0, \tag{46}$$

with a unique positive solution

$$v_1^* = \frac{\lambda - \mu + \sqrt{(\lambda+\mu)^2 + 4\mu}}{2(\lambda+1)}. \tag{47}$$

The presence of any $\mu > 0$ prevents the solution $v_1(\tau)$ from vanishing since the exponential term in the integral of equation (35) contains the integral of $\mu/v_1(\tau)$, which diverges in the limit of vanishing $v_1(\tau)$ and annihilates the exponential. Thus $v_1(\tau)$ may not decrease any further and stays positive.

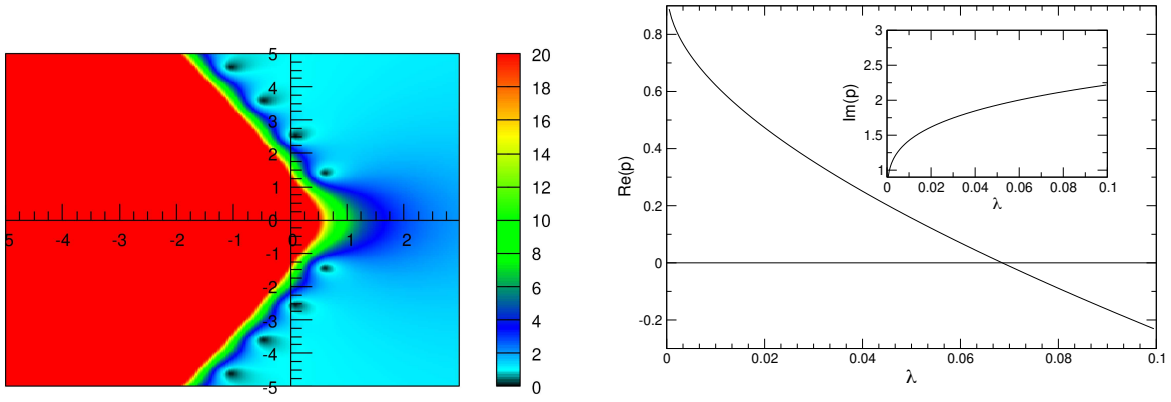

(a) (b)

Figure 8: (a) Surface plot of the amplitude $|1+2\hat{F}(p)|$ for $\lambda = 0.01$ and $\mu = 0$ in the complex plane $(\mathrm{Re}\, p, \mathrm{Im}\, p)$. All values greater than 20 are colored in red. It is shown that for this value of λ, there exist two zeros and their conjugates with positive real parts. (b) Plot of the complex solution of $1+2\hat{F}(p)=0$ with the largest real part as a function of λ.

2.2.4. Stability around the constant solution. The previous solution remains stable provided that any perturbation diminishes with time. As before, we consider a perturbation $\epsilon(\tau)$ such that $v_1(\tau) = v_1^* + \epsilon(\tau)$. After linearizing equation (35) and set $\alpha = 1 + \lambda + \mu/v_1^*$, one obtains the following linear integral equation for $\epsilon(\tau)$:

$$\epsilon(\tau) = -2\int_0^\tau d\tau' \frac{\epsilon(\tau')e^{-2\alpha(\tau-\tau')}}{\left(1-\int_0^{\tau-\tau'} d\tau'' e^{-\alpha\tau''}\right)^3} - 2\frac{\mu}{v_1^*}\int_0^\tau d\tau' \frac{e^{-2\alpha(\tau-\tau')}}{\left(1-\int_0^{\tau-\tau'} e^{-\alpha\tau''}d\tau''\right)^3} \times \left[2\int_{\tau'}^\tau d\tau''\epsilon(\tau'') + 3\frac{\int_{\tau'}^\tau d\tau'' e^{-\alpha(\tau-\tau'')}\int_{\tau''}^\tau d\tau'''\epsilon(\tau''')}{1-\int_0^{\tau-\tau'} d\tau'' e^{-\alpha\tau''}}\right]. \quad (48)$$

This integral equation resists simplification via a Laplace transform as before. Instead, we consider a perturbation of the form $\epsilon(\tau) = \epsilon_0 e^{\Omega\tau}$, where ϵ_0 is a small amplitude and Ω is the complex frequency. If the real part is negative ($\mathrm{Re}\,\Omega < 0$), the perturbation is irrelevant having the constant solution stable. Otherwise we expect some oscillatory behavior with frequency $\mathrm{Im}\,\Omega$. The equation for the complex frequency Ω reads

$$1 + 2J_3(2\alpha+\Omega,\alpha) + \frac{2\mu}{\Omega v_1^*}\Big\{2\Big[J_3(2\alpha,\alpha) - J_3(2\alpha+\Omega,\alpha)\Big] + \frac{3}{\alpha}\Big[J_4(2\alpha,\alpha) - J_4(3\alpha,\alpha)\Big] - \frac{3}{\alpha+\Omega}\Big[J_4(2\alpha,\alpha) - J_4(3\alpha+\Omega,\alpha)\Big]\Big\} = 0, \quad (49)$$

which reduces, via some algebra, to

$$\Omega(1+\lambda+\Omega)\Phi(1-\alpha,1,1-\Omega/\alpha) - \frac{\pi\Omega(1+\lambda+\Omega)(\alpha-1)^{\Omega/\alpha}}{(\alpha-1)\sin(\pi\Omega/\alpha)} + \frac{\Omega^2+(1+\lambda+\alpha)\Omega}{\alpha+\Omega} + \frac{\alpha(\alpha^2\lambda-(1+\lambda)\alpha+1+\lambda)}{(\alpha-1)^2(\alpha+\Omega)} = 0, \tag{50}$$

with $\alpha = 1+\lambda+\mu/v_1^*$. When $\mu = 0$ or $\alpha = 1+\lambda$, equation (44) is recovered.

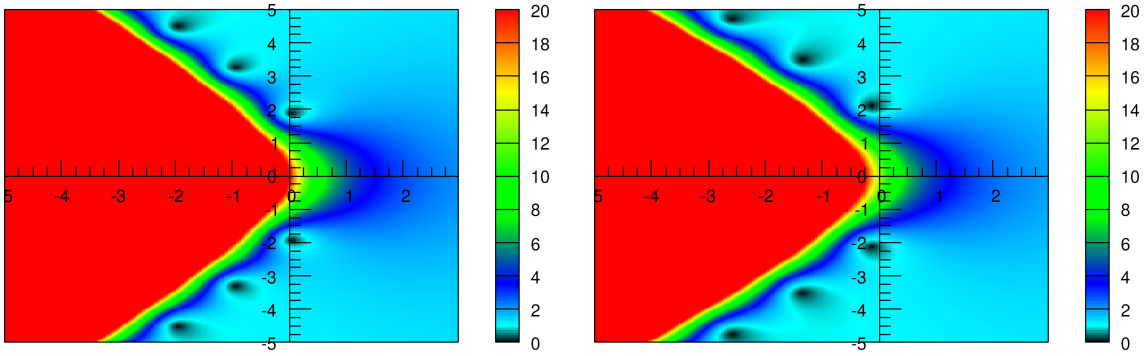

(a) (b)

Figure 9: Surface plot of the modulus of equation (50) in the complex Ω-plane $(\mathrm{Re}\,\Omega, \mathrm{Im}\,\Omega)$, for $\mu = 10^{-4}$ and $\lambda =$ (a) 0.05 and (b) 0.08. In (a), there exists one conjugate pair of Ω with a positive real part.

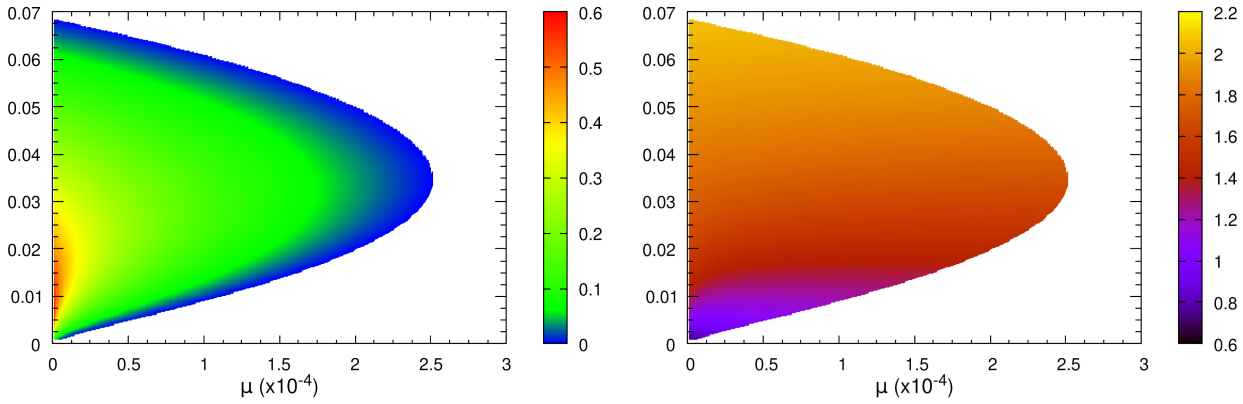

(a) (b)

Figure 10: (a) Phase diagram in the plane (λ, μ), depicting (a) the real part and (b) the imaginary part of the solution of equation (50) for which the real part $\mathrm{Re}\,\Omega(>0)$ is the largest.

In figure 9, we plot the the modulus of equation (50) in the complex Ω-plane. When $\lambda = 0.08$ shown in (b), all zeros locate on the left part of the plane with negative real parts. For $\lambda = 0.05$

in (a), only one conjugate pair of Ω has a strictly positive real part. Figure 10 presents (a) the phase diagram in the plane (λ, μ) for which the zero with the largest real part is positive, together with (b) the corresponding frequency values. When the real part is positive ($\mathrm{Re}\,\Omega > 0$), the perturbation is relevant and oscillations occur for any value of (λ, μ) in the colored domain except for $\mu = 0$ where v_1 vanishes at some finite time. However for any nonzero value of μ, v_1 does not vanish due to the term μ/v_1 in the integral of equation (35) and the oscillations are restricted to a zone for which μ is no larger than 2.5×10^{-4}. Outside the colored area of figure 10(a), the perturbation is irrelevant and v_1 approaches its limiting value v_1^*.

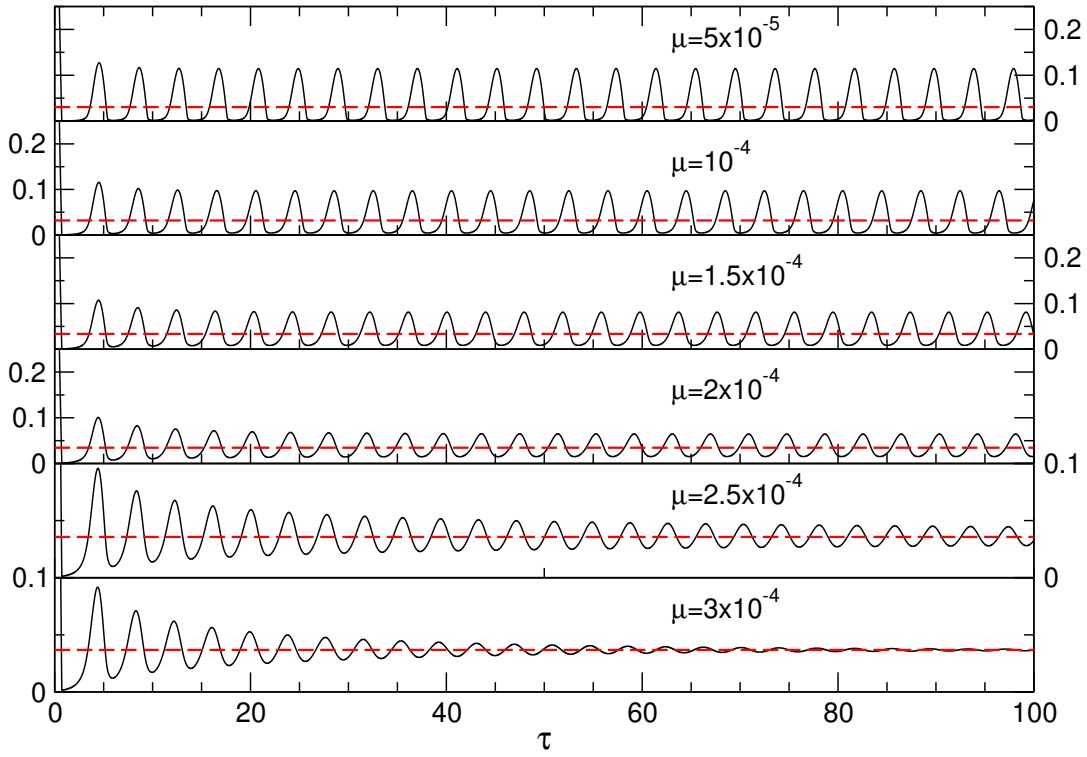

Figure 11: Time evolution of $v_1(\tau)$ for $N = 10000$, $\lambda = 0.03$, and several values of μ. For $\mu = 2.5 \times 10^{-4}$, the oscillations are slowly damped and for $\mu = 3 \times 10^{-4}$ the oscillations disappear and v_1 approaches asymptotically v_1^* (red dashed lines).

Table 2: Frequency $\Omega_{\rm num}$ for $\lambda = 0.6$ and several values of μ, extracted from the Fourier transform of the time oscillations in figure 6. For comparison, the imaginary part $\mathrm{Im}\,\Omega$ of the solution of equation (26) is also given.

μ	$\Omega_{\rm num}$	$\mathrm{Im}\,\Omega$
5×10^{-5}	1.548	1.684
1×10^{-4}	1.573	1.655
1.5×10^{-4}	1.594	1.640
2×10^{-4}	1.612	1.632
2.5×10^{-4}	1.627	1.628

3. Discussion

We have shown that oscillations are present in both sets of exponent $(a, b) = (1, 0)$ and $(1, 1)$, but with different amplitudes for the parameters λ and μ. The oscillator equations (15) and (35) can be put into the generalized form:

$$v_1(\tau) = 1 - 2\int_0^\tau d\tau' \frac{v_1(\tau')\exp\left[-\beta(\tau-\tau') - 2\mu\int_{\tau'}^\tau d\tau'' v_1^{-1}(\tau'')\right]}{\left[1 - \int_{\tau'}^\tau d\tau'' \exp[(-\alpha(\tau-\tau'') - \mu\int_{\tau''}^\tau d\tau''' v_1^{-1}(\tau'''))]\right]^3}, \tag{51}$$

with the parameters

$$\begin{aligned}(a,b) = (1,0):&\ \alpha = 1 \text{ and } \beta = 2+\lambda,\\ (a,b) = (1,1):&\ \alpha = 1+\lambda \text{ and } \beta = 2+2\lambda.\end{aligned} \tag{52}$$

The denominator in the integral is important in the presence of oscillating solutions. One simple counterexample is the following class of integral equations

$$v_1(\tau) = 1 - 2\int_0^\tau d\tau' v_1(\tau')\exp\left[-\beta(\tau-\tau') - 2\mu\int_{\tau'}^\tau d\tau'' v_1^{-1}(\tau'')\right], \tag{53}$$

with $\beta > 0$ for simplicity. From this integral equation, we obtain, via differentiation and reorganization of different terms, a simple first-order ODE:

$$\frac{dv_1(\tau)}{d\tau} = -(2+\beta)v_1(\tau) + \beta - 2\mu + 2\frac{\mu}{v_1(\tau)}, \tag{54}$$

which has the positive asymptotic constant solution

$$v_1^* = \frac{\beta - 2\mu + \sqrt{(\beta+2\mu)^2 + 16\mu}}{2(2+\beta)}. \tag{55}$$

Again we can probe the stability of this solution by considering the exponential perturbation $v_1(\tau) = v_1^* + \epsilon(\tau)$ with $\epsilon(\tau) = \epsilon_0 e^{\Omega\tau}$. A lengthy but straightforward calculation leads to the unique real negative solution

$$\Omega = -(2+\beta) - \frac{2\mu}{v_1^*} - \frac{4\mu}{v_1^*\beta + 2\mu}\,(<0), \tag{56}$$

which implies that the class of integral equations (53) has no asymptotic solution other than the constant solution given by equation (55). It is easy to see that for $\mu = 0$, the solution of equation (54), which is given by $v_1(\tau) = (2+\beta)^{-1}(2e^{-(2+\beta)\tau} + \beta)$, decays exponentially towards v_1^* with $\Omega = -(2+\beta) < 0$. In general, one can examine the stability of equation (51) for any α and β, to generalize equations (26) and (49) for the complex frequency Ω:

$$1 + 2J_3(\bar{\beta}+\Omega, \bar{\alpha}) + 2\frac{\mu}{\Omega v_1^*}\Big\{2\Big[J_3(\bar{\beta}, \bar{\alpha}) - J_3(\bar{\beta}+\Omega, \bar{\alpha})\Big] + \frac{3}{\bar{\alpha}}\Big[J_4(\bar{\beta}, \bar{\alpha}) - J_4(\bar{\beta}+\bar{\alpha}, \bar{\alpha})\Big] - \frac{3}{\bar{\alpha}+\Omega}\Big[J_4(\bar{\beta}, \bar{\alpha}) - J_4(\bar{\beta}+\bar{\alpha}+\Omega, \bar{\alpha})\Big]\Big\} = 0, \tag{57}$$

with $\bar{\alpha} \equiv \alpha + \mu/v_1^*$ and $\bar{\beta} \equiv \beta + 2\mu/v_1^*$, where v_1^* is the constant solution of equation (51) and satisfies the implicit equation

$$v_1^{*-1} = 1 + 2J_3(\bar{\beta}, \bar{\alpha}). \tag{58}$$

For a general set of exponents (a, b), it is not obvious how to obtain a general oscillator equation when a or b can take fractional values. In this case, we can nevertheless generalize equation (4) for the moments φ_r to any real number r:

$$\frac{\partial \varphi_r}{\partial \tau} = -\left(1 + \frac{\mu}{v_1}\right)\varphi_{r+a} - \lambda\varphi_{r+b} + \sum_{j=0}^{\infty}\binom{r+a}{j}\varphi_j + 2^{r+a}v_1. \tag{59}$$

It is then convenient to introduce the set of generating functions with positive integers (l, m, n):

$$G_{mn}(u, \tau) = \sum_{l=0}^{\infty}\frac{u^l}{l!}\varphi_{l+ma+nb}, \tag{60}$$

since equation (59) should generate via recursion all possible moments with $r = l + ma + nb$, which form a set of closed indices for the equation. While initial conditions are given by $G_{mn}(u, 0) = 0$, we are interested in the first component $G_{00}(0, \tau) = G(0, \tau) = \varphi_0 = 1 - v_1$. Multiplying equation (59) by $u^l/l!$ and summing over l with $r = l + ma + nb$, we obtain

$$\frac{\partial G_{mn}}{\partial \tau} = -(1 + \mu/v_1)G_{m+1n} - \lambda G_{mn+1} + 2^{(m+1)a+nb}e^{2u}v_1 + \sum_{l=0}^{\infty}\frac{u^l}{l!}\sum_{j=0}^{\infty}\binom{l+(m+1)a+nb}{j}\varphi_j, \tag{61}$$

where the double sum may be evaluated through the use of the Egorychev method as in equation (7):

$$\sum_{l\geq 0}\frac{u^l}{l!}\sum_{j\geq 0}\binom{l+(m+1)a+nb}{j}\varphi_j = \sum_{l\geq 0}\frac{u^l}{l!}\sum_{j\geq 0}\oint\frac{dz}{2i\pi z}\frac{(1+z)^{l+(m+1)a+nb}}{z^j}\varphi_j. \tag{62}$$

This yields

$$\sum_{l\geq 0}\frac{u^l}{l!}\sum_{j\geq 0}\binom{l+(m+1)a+nb}{j}\varphi_j = \sum_{j\geq 0}\oint\frac{dz}{2i\pi z}\frac{(1+z)^{(m+1)a+nb}}{z^j}e^{u(1+z)}\varphi_j$$

$$= \sum_{l\geq 0}\sum_{j\geq l} e^u \binom{(m+1)a+nb}{l} \frac{u^{j-l}}{(j-l)!}\varphi_j$$
$$= e^u \sum_{l\geq 0} \binom{(m+1)a+nb}{l} \frac{\partial^l G_{00}(u,\tau)}{\partial u^l}, \qquad (63)$$

which leads equation (61) to obtain the closed form:

$$\frac{\partial G_{mn}}{\partial \tau} = -(1+\mu/v_1)G_{m+1n} - \lambda G_{mn+1} + 2^{(m+1)a+nb}e^{2u}v_1 + e^u \sum_{l\geq 0} \binom{(m+1)a+nb}{l} \frac{\partial^l G_{00}}{\partial u^l}. \qquad (64)$$

The last sum can formally be identified as the derivation operator $(1+\partial_u)^\gamma$ with $\gamma = (m+1)a+nb$. In the previous analysis with $(a,b) = (1,0)$ and $(a,b) = (1,1)$, see equations (5) and (29), we have, for $(m,n) = (0,0)$, $\gamma = 1$, and therefore the operator gives simply the terms $e^u(G_{00} + \partial_u G_{00})$. In the general case of a and b integers, we obtain the following linear partial differential equation with non-constant coefficients:

$$\frac{\partial G_{00}}{\partial \tau} = -(1+\mu/v_1)\frac{\partial^a G_{00}}{\partial u^a} - \lambda \frac{\partial^b G_{00}}{\partial u^b} + 2^a e^{2u} v_1 + e^u \left(1 + \frac{\partial}{\partial u}\right)^a G_{00},$$

which is in general unsolvable by means of characteristics curves, except for the cases treated in the previous sections.

4. Conclusion

In this paper, we have investigated the dynamics of an infinite set of clusters interacting with monomers leading to aggregation or coagulation with rate k^a or fragmentation with rate λk^b, depending on the mass k of the cluster. This usually leads to an equilibrium state, but we have shown that the addition of a self-disintegration process with rate μk^b can induce oscillations in the cluster densities for a restricted domain of parameters (λ, μ), where μ can be infinitely small. The cluster density v_k is solely a function of the monomer density v_1, and the latter is determined implicitly by a time integral equation in the form of equation (51). This implicit equation always possesses a non-zero constant solution in the long-time limit. If we perturb this solution with any arbitrary complex exponential growth, its stability depends on the location of the exponential rate Ω in the complex plane and satisfying a general equation equation (57). If the real part of all admissible solutions Ω is negative, the constant solution is stable. Otherwise, if a finite set of Ω conjugates have positive real parts, oscillations occur with a frequency slightly different than the imaginary part of the solutions Ω that has the largest real part. This difference is negligible on the boundary of the domain of oscillations when $\mathrm{Re}\,\Omega = 0$, and increases with $\mathrm{Re}\,\Omega > 0$. However, we cannot extract from the function (57) the exact oscillation frequency since the integral equation (51) is highly nonlinear. Corrections to the estimated frequency can be made through the use of standard techniques [27] that can be applied if we know the existence of an ODE for v_1, see [23]

in the case of the Liénard mechanism. However, there is no obvious ODE of finite order derivable from equation (51) through consecutive differentiation and recursive substitutions in a controllable manner. We also notice that oscillations can occur in finite systems even if they vanish in the limit of the system size $N \to \infty$, see figures 2 and 3. This is due to the variations with N of the location of the solutions of equation (57) in the complex plane.

Acknowledgments

This work was supported by the National Research Foundation of Korea through the Basic Science Research Program (Grant No. 2022R1A2C1012532).

References

[1] Krapivsky P L, Redner S and Ben-Naim E 2010 *A Kinetic View of Statistical Physics* (New York: Cambridge University Press)
[2] Cuzzi J N, Burns J A, Charnoz S, Clark R N, Colwell J E, Dones L, Esposito L W, Filacchione G, French R G, Hedman M M, Kempf S, Marouf E A, Murray C D, Nicholson P D, Porco C C, Schmidt J, Showalter M R, Spilker L J, Spitale J N, Srama R, Sremčević M, Tiscareno M S and Weiss J 2010 *Science* **327** 1470–1475
[3] Brilliantov N, Krapivsky P L, Bodrova A, Spahn F, Hayakawa H, Stadnichuk V and Schmidt J 2015 *Proc. Nat. Acad. Sci.* **112** 9536–9541
[4] Brilliantov N V, Formella A and Pöschel T 2018 *Nat. Commun.* **9** 797
[5] White H W 1981 *J. Colloid Interface Sci.* **87** 204–208
[6] Ziff R M, McGrady E D and Meakin P 1985 *J. Chem. Phys.* **82** 5269–5274
[7] Hayakawa H 1987 *J. Phys. A* **20** L801–L805
[8] Hayakawa H and Hayakawa S 1988 *Publ. Astron. Soc. Japan* **40** 341–345
[9] Vigil R D, Ziff R M and Lu B 1988 *Phys. Rev. B* **38** 942
[10] Wattis J A 2006 *Physica D* **222** 1–20
[11] Krapivsky P L, Otieno W and Brilliantov N V 2017 *Phys. Rev. E* **96** 042138
[12] da Costa F P 2015 Mathematical Aspects of Coagulation-Fragmentation Equations *Math. Energy Clim. Chang.* ed Bourguignon J P, Jeltsch R, Pinto A and Viana M (Springer) pp 83–162 CIM Series ed
[13] Bodrova A S, Stadnichuk V, Krapivsky P L, Schmidt J and Brilliantov N V 2019 *J. Phys. A Math. Theor.* **52** 205001
[14] Brilliantov N V, Otieno W and Krapivsky P L 2021 *Phys. Rev. Lett.* **127** 250602
[15] Ball R C, Connaughton C, Jones P P, Rajesh R and Zaboronski O 2012 *Phys. Rev. Lett.* **109** 168304
[16] Matveev S A, Krapivsky P L, Smirnov A P, Tyrtyshnikov E E and Brilliantov N V 2017 *Phys. Rev. Lett.* **119**(26) 260601
[17] Connaughton C, Dutta A, Rajesh R, Siddharth N and Zaboronski O 2018 *Phys. Rev. E* **97** 022137 (*Preprint* `arXiv:1710.01875`)
[18] Pego R L and Velázquez J J 2020 *Nonlinearity* **33** 1812–1846 (*Preprint* `arXiv:1905.02605`)
[19] Słomka J and Stocker R 2020 *Phys. Rev. Lett.* **124**(25) 258001
[20] Budzinskiy S S, Matveev S A and Krapivsky P L 2021 *Phys. Rev. E* **103** L040101 (*Preprint* `arXiv:2012.09003`)
[21] Kalinov A, Osinsky A I, Matveev S A, Otieno W and Brilliantov N V 2022 *J. Comput. Phys.* **467** 111439
[22] Niethammer B, Pego R L, Schlichting A and Velázquez J J L 2022 *SIAM J. Appl. Math.* **82** 1194–1219
[23] Fortin J Y 2022 *J. Phys. A: Math. Theor.* **55** 485003

[24] Buchstaber V M and Bunkova E Y 2012 Algebraically Integrable Quadratic Dynamical Systems (*Preprint* `arXiv:1212.6675`)
[25] Calogero F, Conte R and Leyvraz F 2020 *J. Math. Phys.* **61** 102704
[26] Dorogovtsev S N and Mendes J F F 2002 *Adv. Phys.* **51** 1079–1187 (*Preprint* `arXiv:0106144`)
[27] Nayfeh A H and Mook D T 1995 *Nonlinear Oscillations* Wiley Classics Library (New York: Wiley)